XIV Ulusal Medikal Fizik Kongresi
21-24 Kasım 2013 Kervansaray Lara Convention Center/ANTALYA

SRS UYGULAMALARINDA TUMOR BÖLÜTLEMESİ; KONTRAST MADDE VERİLEN MR GÖRÜNTÜLERİNİN SEGMENTASYONU

Med. Fiz. Uzm. Nadir KÜÇÜK
Özel Anadolu Sağlık Merkezi
24 Kasım 2013

Tumor-Cut: Segmentation of Brain Tumors on Contrast Enhanced MR Images for Radiosurgery Applications

Andac Hamamci*, Nadir Kucuk, Kutlay Karaman, Kayihan Engin, and Gozde Unal, *Senior Member, IEEE*

GİRİŞ

Manuscript received September 12, 2011; revised December 08, 2011; accepted December 14, 2011. Date of publication December 26, 2011; date of current version March 02, 2012. This research was supported by Tubitak Research Grant 108E126, and Marie Curie International Reintegration Grant PIRG03-GA-2008-231052 within the 7th European Community Framework Programme. *Asterisk indicates corresponding author.*

*A. Hamamci is with the Faculty of Engineering and Natural Sciences at the Sabanci University, 34956 Istanbul, Turkey (e-mail: andachamamci@sabanci-univ.edu).

G. Unal is with the Faculty of Engineering and Natural Sciences at the Sabanci University, 34956 Istanbul, Turkey (e-mail: gozdeunal@sabanci-univ.edu).

N. Kucuk and K. Engin are with the Department of Radiation Oncology at the Anadolu Medical Center, 41400 Kocaeli, Turkey (e-mail: nadir.kucuk@anadolusaglik.org; kayihan.engin@anadolusaglik.org).

K. Karaman is with the Department of Radiology at the Anadolu Medical Center, 41400 Kocaeli, Turkey (e-mail: kutlay.karaman@anadolusaglik.org).

Digital Object Identifier 10.1109/TMI.2011.2181857

GİRİŞ

- **SRS uygulamalarında konturlama genellikle T1 ağırlıklı MR görüntüleri ile elde ediliyor.**
- **Manuel konturlama yapılıyor.**
- **Gadolinium kontrast maddesi hastaya verildiğinde kan beyin bariyerini geçebilen madde, damar ve tümörü yüksek yoğunlukta göstererek görünür hale getirir.**
- **Beyin tümörlerini segmente etmeye çalışan birçok yöntem vardır.**

GİRİŞ

- **Tümörü, infiltrasyonu ve ödemi göstermek için birçok MR tekniği var.**

-Perfüzyon
-Düfüzyon
-Spektroskopi

- **Bu tekniklerin tamamı T1 ve T2 'ye göre düşük rezülüsyonlu görüntüler vermekte ve segmentasyon zorlaşmakta.**

- **T2 ağırlıklı görüntülerde ödemi görüntülmekte.**

GİRİŞ

- **Tümör segmentasyonu için birçok matematiksel algoritma var ve proses zamanları önemli bir parametre**

- **Bu çalışmada Cellular Automata (CA) algoritması graph-theoratic metodu ile ilişkilendirilip uygun geçiş kuralları ile en kısa yolu bulup çözümleme yapılması amaçlanmıştır.**

GİRİŞ

II. Background

A. Seeded Image Segmentation

Given an undirected graph $G = (V, E)$ with vertices $v \in V$ and edges $e \in E$, a weighted graph assigns a value w_{ij} (typically real and nonnegative) to each edge e_{ij} between vertices v_i and v_j. In image segmentation problems, vertices are corresponding to image pixels, while edge weights are similarity measures between neighboring pixels based on image features (e.g., intensities). Each vertex v_i has an attribute x_i, which is an indicator of the probability of a label (e.g., a foreground and a background label). With the foreground F and background B seeds supplied by the user, the labeling problem is solved by

$$x^{\text{opt}} = \arg\min_{x} \left[\sum_{e_{ij} \in E} (w_{ij}|x_i - x_j|)^q \right]^{\frac{1}{q}}$$
$$\text{s.t. } x(F) = 1, \quad x(B) = 0 \quad (1)$$

TUMOR CUT

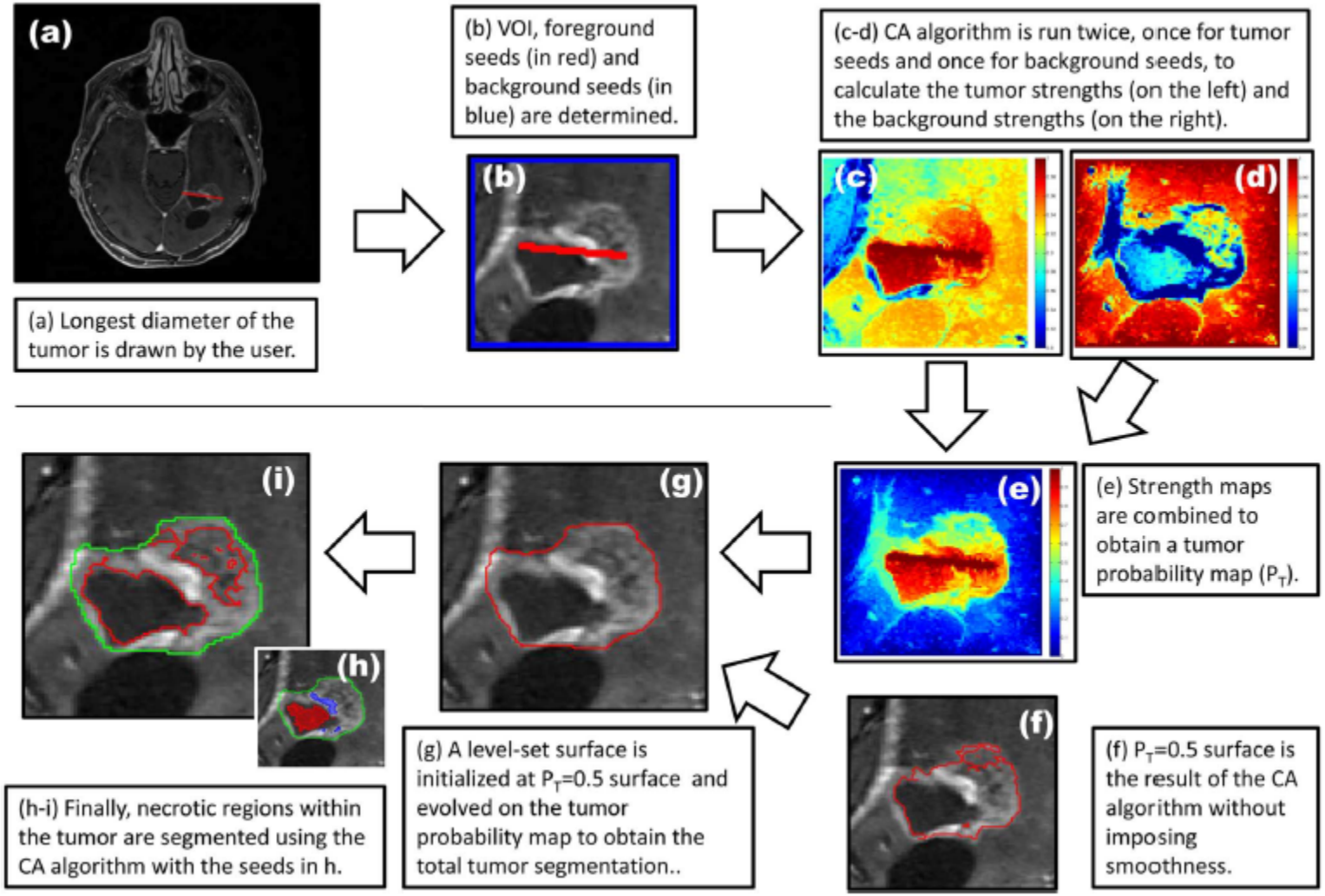

Fig. 1. Steps of the proposed tumor segmentation method (see text for explanations).

TUMOR CUT

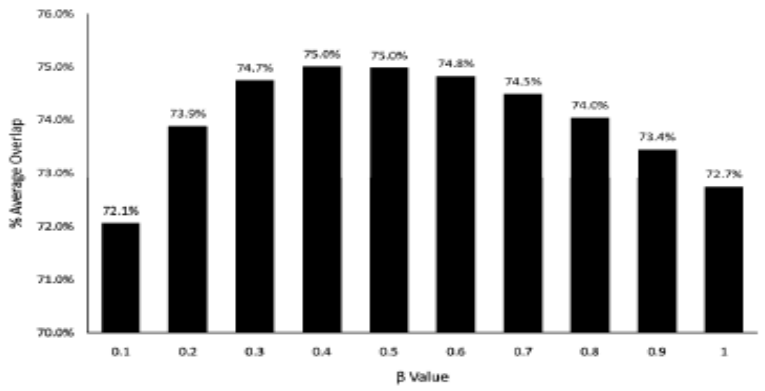

Fig. 3. Effect of β on the segmentation performance.

regions to tumor region, which are usually surrounded by enhanced tissue. Finally, it is possible to exclude nearby vascular structures that are enhanced by administration of the contrast agent.

CA algorithm has the advantage of finding distance of each cell to the nearest seed in a simultaneous iteration. However, the resulting strength map has only one-sided information, that is the distance to the other label classes is not available. In order to create a probabilistic map, which can be used in an active surface (e.g., a level set surface) evolution, the algorithm is run for each class with corresponding class seeds (tumor and healthy) separately. Geodesic distances to the class seeds can be calculated by $D = -\ln(x)$. Therefore, the tumor probability map is obtained by combining the distances for tumor (D_T) and background (D_B) as

$$P_{\text{Tumor}} = \frac{D_B}{D_T + D_B}. \quad (6)$$

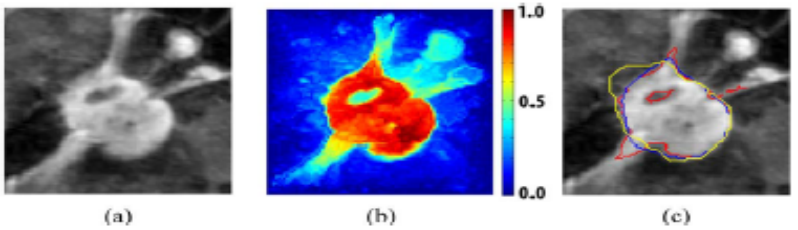

Fig. 4. Effect of smoothing. Example of tumor slice with vascularization and necrotic part (a). Tumor probability map obtained by CA algorithm (b). Segmentation result before smoothing (red), after smoothing (blue), and expert (yellow) (c).

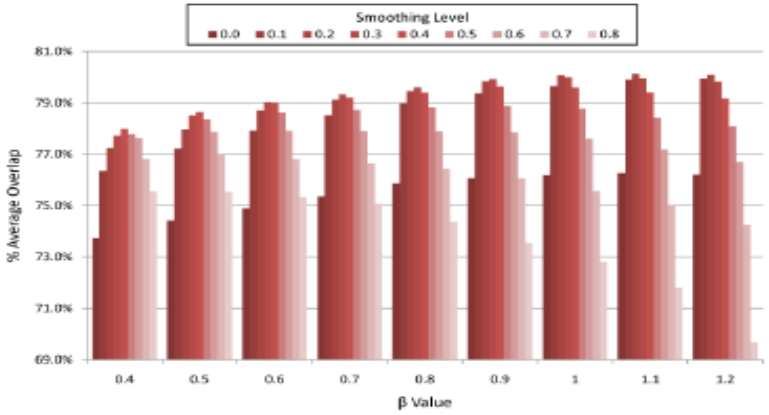

Fig. 5. Effect of β for different smoothing levels (increasing from dark to light) on the average dice overlap performance on our clinical data set.

validation studies. As a result, our interactive tumor segmentation includes an appropriate intelligent smoothing of the tumor borders based on the labeling results obtained from a graph-theoretic approach. This is a process that is expected to simulate the expert's manual contouring. The qualitative effect

TUMOR CUT

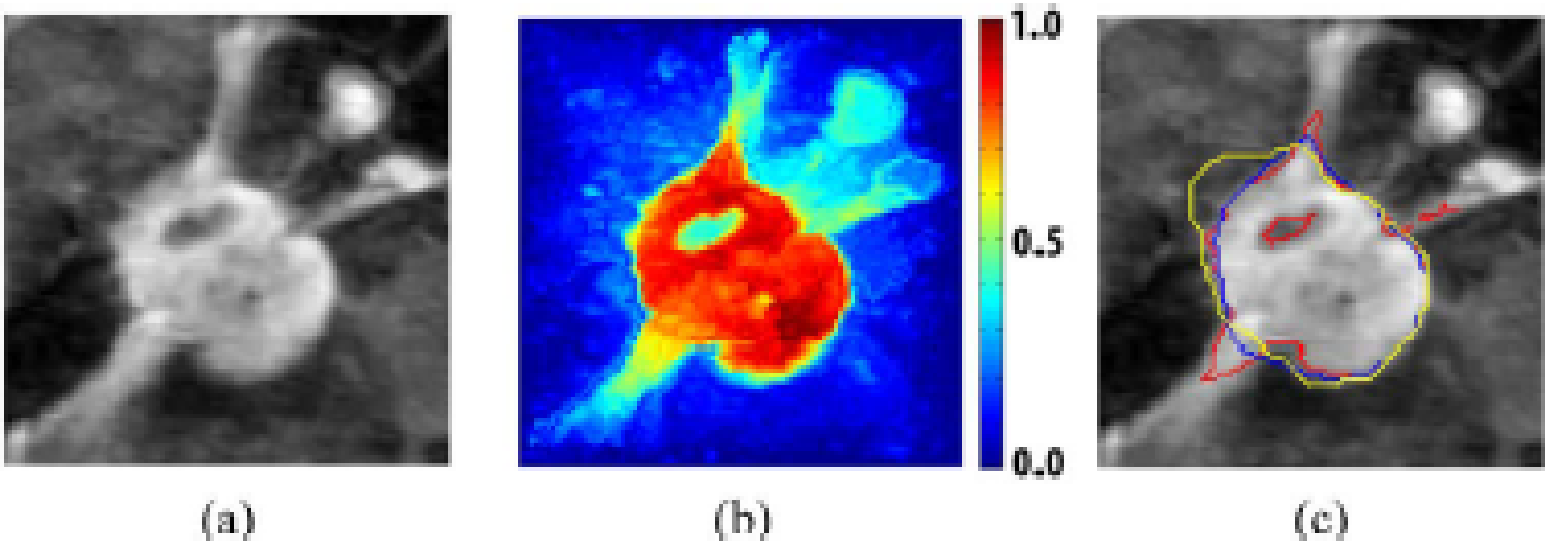

Fig. 4. Effect of smoothing. Example of tumor slice with vascularization and necrotic part (a). Tumor probability map obtained by CA algorithm (b). Segmentation result before smoothing (red), after smoothing (blue), and expert (yellow) (c).

Tümör olasılığı

lated by $D = -\ln(x)$. Therefore, the tumor probability map is obtained by combining the distances for tumor (D_T) and background (D_B) as

$$P_{\text{Tumor}} = \frac{D_B}{D_T + D_B}. \quad (6)$$

NEKROTİK VE KONTRASTLANMA EŞİK DEĞERİ

$$\sum_{I=0}^{T_{\text{nec}}} H(I) = 0.25 \cdot N_{\text{nec}}^{\text{OTSU}} \text{ and } \sum_{I=T_{\text{enh}}}^{I_{\max}} H(I) = 0.25 \cdot N_{\text{enh}}^{\text{OTSU}} \quad (7)$$

where H is the volume intensity histogram, $N_{\text{nec}}^{\text{OTSU}}$ and $N_{\text{enh}}^{\text{OTSU}}$ are rough volumes estimated with Otsu's method and T_{nec} and T_{enh} are the necrotic and enhanced thresholds.

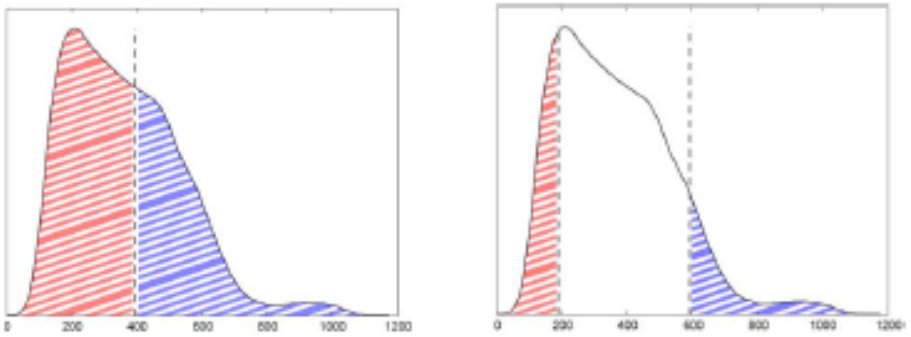

(a) (b)

Fig. 7. (a) Segmentation with a single threshold. (b) Necrotic and enhanced thresholds to determine initial seeds.

SONUÇ

			TEDAVİ ÖNCESİ				TEDAVİ SONRASI		
Hasta No	Prot ID	Tümör Hacmi (mm^3)	Nekrotik Hacim (mm^3)	En Büyük Çap (mm)	Nekrotik Oranı (%)	Tümör Hacmi (mm^3)	Nekrotik Hacim (mm^3)	En Büyük Çap (mm)	Nekrotik Oranı (%)
1	144954	6796,5	2031,2	27,2	29,9%	7503,9	2038,6	30,7	27,2%
2	16420	2805,9	678,6	24,8	24,2%	2858,1	581,4	24,3	20,3%
3	44991	16055,4	1712,5	34,6	10,7%	20089,3	5915,6	36,8	29,4%
4	57984	3641,6	1155,6	25,8	31,7%	3642,0	1206,8	25,1	33,1%
5	121818	953,3	94,2	16,3	9,9%	961,9	73,3	16,5	7,6%
6	1422	6891,7	1604,2	35,8	23,3%	14565,8	5233,9	45,9	35,9%
7	92346	15342,6	6714,5	39,2	43,8%	20578,9	7244,6	44,5	35,2%
8	6639	4114,1	1106,1	31,1	26,9%	3755,1	895,8	30,6	23,9%
9	185354	1204,9	160,5	19,8	13,3%	1101,8	231,5	19,8	21,0%
10	183660	4263,3	947,7	21,9	22,2%	5727,6	1447,1	29,0	25,3%
11	22557	16382,6	7147,7	44,3	43,6%	23117,0	9512,1	46,2	41,1%
12	11592	18496,5	10461,6	38,6	56,6%	16933,0	7311,1	42,5	43,2%
13	2995	601,9	127,7	15,0	21,2%	766,6	221,4	16,1	28,9%
14	175884	11573,0	1367,6	36,3	11,8%	19148,3	6035,6	44,3	31,5%
15	132120	10114,0	266,1	31,2	2,6%	9237,8	824,0	28,7	8,9%
16	133478	7224,8	2379,6	28,4	32,9%	7603,9	2318,8	28,6	30,5%

SONUÇ

		Dice Overlap (%)	Volume Err.(%)	Maximum Dist.(mm)	Mean Dist.(mm)	Median Dist.(mm)
Tumor 1	Glioblastoma Multiforme	70.2 ± 7.3	24.3 ± 13.0	5.1 ± 1.0	1.0 ± 0.6	0.7 ± 0.4
Tumor 2	Acoustic Neuroma	76.2 ± 1.8	27.6 ± 8.4	10.2 ± 0.5	2.3 ± 0.2	1.2 ± 0.1
Tumor 3	Astrocytoma Grade 2-3	80.3 ± 5.7	27.1 ± 10.4	7.7 ± 1.2	1.8 ± 0.3	1.6 ± 0.2
Tumor 4	Brain Metastasis	80.9 ± 0.6	31.0 ± 2.4	3.4 ± 0.1	1.1 ± 0.0	1.1 ± 0.0
Tumor 5	Brain Metastasis	77.6 ± 0.5	34.6 ± 0.8	4.7 ± 0.1	1.1 ± 0.0	1.1 ± 0.0
Tumor 6	Brain Metastasis	83.3 ± 0.3	24.7 ± 1.0	4.6 ± 0.5	1.2 ± 0.0	1.1 ± 0.0
Tumor 7	Acoustic Neuroma	68.2 ± 1.2	46.4 ± 1.7	3.5 ± 0.4	1.0 ± 0.1	1.1 ± 0.0
Tumor 8	Glioblastoma Multiforme	88.2 ± 1.6	8.0 ± 6.6	7.2 ± 1.9	1.1 ± 0.2	0.8 ± 0.1
Tumor 9	Brain Metastasis	84.6 ± 0.6	16.9 ± 2.0	5.9 ± 0.5	0.9 ± 0.1	0.7 ± 0.0
Tumor 10	Astrocytoma Grade 2-3	90.3 ± 1.1	6.8 ± 4.4	5.4 ± 2.1	0.8 ± 0.2	0.6 ± 0.0
Tumor 11	Meningioma	82.4 ± 1.2	19.5 ± 2.7	12.1 ± 0.7	2.1 ± 0.1	1.2 ± 0.0
Tumor 12	Acoustic Neuroma	84.0 ± 0.4	16.1 ± 4.8	2.1 ± 0.2	0.5 ± 0.0	0.5 ± 0.0
Tumor 13	Brain Metastasis	65.9 ± 1.4	44.9 ± 3.3	5.0 ± 0.7	1.6 ± 0.1	1.5 ± 0.0
Tumor 14	Glioblastoma Multiforme	77.8 ± 4.7	16.6 ± 16.2	9.5 ± 3.1	2.5 ± 0.9	1.9 ± 0.6
Tumor 15	Meningioma	87.7 ± 1.6	10.1 ± 4.0	3.3 ± 0.2	0.6 ± 0.1	0.5 ± 0.0
Tumor 16	Meningioma	86.8 ± 0.7	4.6 ± 2.6	3.4 ± 0.6	0.8 ± 0.0	0.5 ± 0.0
Tumor 17	Meningioma	72.4 ± 1.1	26.8 ± 18.3	4.9 ± 0.1	1.2 ± 0.1	1.0 ± 0.1
Tumor 18	Brain Metastasis	81.3 ± 2.4	7.1 ± 6.8	4.8 ± 1.3	1.1 ± 0.2	0.7 ± 0.1
Tumor 19	Brain Metastasis	83.1 ± 0.7	22.1 ± 2.3	2.3 ± 1.5	0.5 ± 0.1	0.5 ± 0.0
Average		80.1 ± 6.9	21.9 ± 12.1	5.5 ± 2.7	1.2 ± 0.6	1.0 ± 0.4

SONUÇ

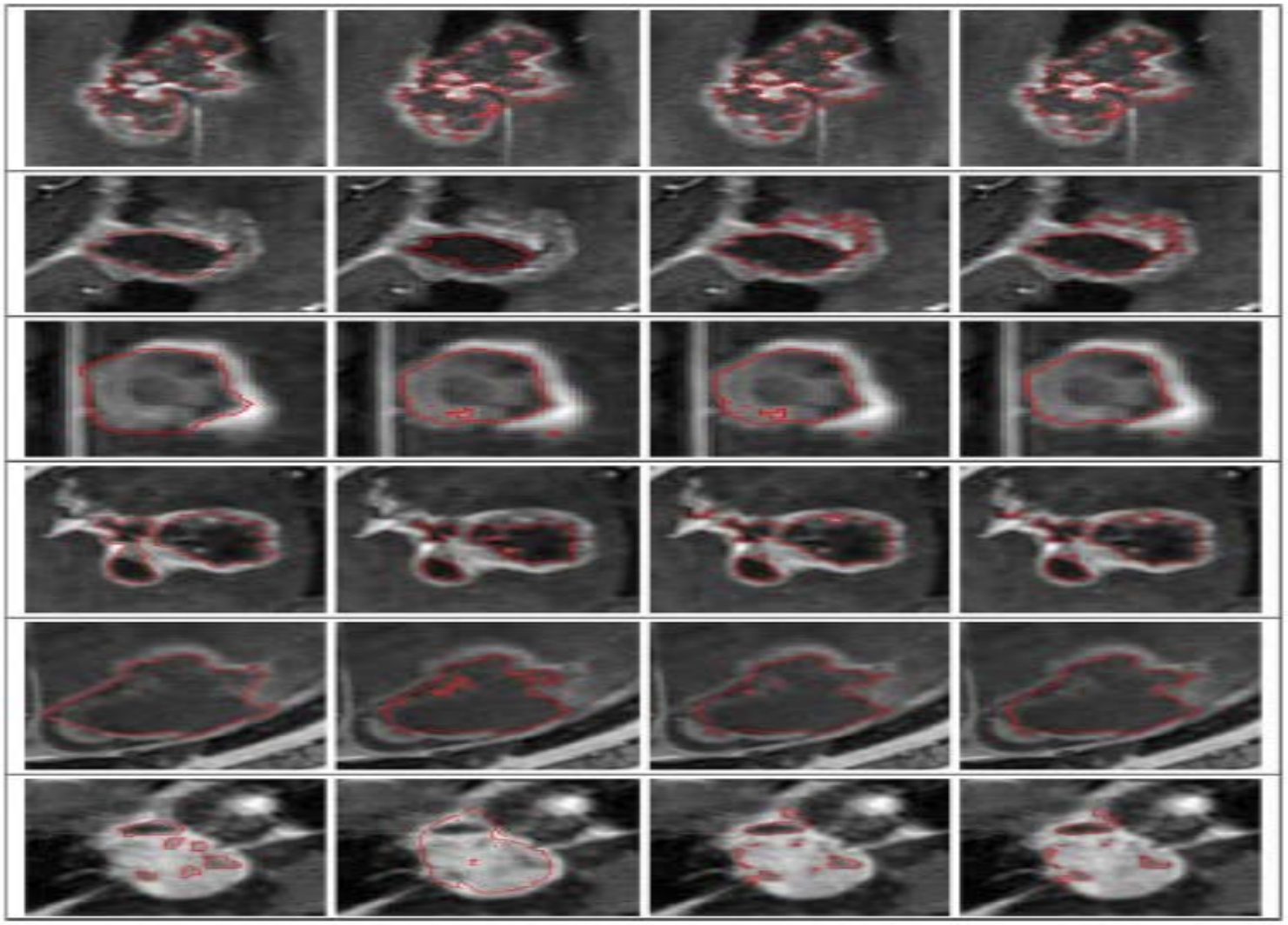

Fig. 17. Necrotic segmentation results for six different tumors on each row. Left-to-right: Manual Expert Delineation; EM Segmentation; Otsu Thresholding; CA Tumor Segmentation.